Asian Journal of Chemistry Vol. 20, No. 3 (2008), 2238-2250

Bubble-Particle Attachment Probability on Coarse Particles Flotation

B. SHAHBAZI† and B. REZAI*
Department of Chemistry, Amirkabir University of Technology, Tehran, Iran
E-mail: brezai1@yahoo.com

In this research, results are reported on the effect of impeller speed and air flow rate on flotation recovery for quartz particles of -590+212 μm. It is found that maximum flotation response was observed at impeller speed of 1100 rpm and 15 L/h air flow rate. For either more quiescent (impeller speed < 1100 rpm) or more turbulent conditions, flotation recovery decreased steadily. Furthermore, amount of attachment probabilities is calculated using suitable equation. According to this study, with decreasing particle size, air flow rate and impeller speed, probability of attachment increased and with increasing contact angle, probability of attachment increased. For various air flow rates, impeller speed and particle size, collision angle has been calculated. Maximum collision angle obtained at 72.82º with 15 L/h air flow rate, particle size of 256 μm and impeller speed of 700 rpm and minimum collision angle obtained at 64º with 45 L/h air flow rate, particle size of 256 μm and impeller speed of 1300 rpm. In this study, maximum attachment angle, θ_{cr}, was 39.33º around 75 L/h air flow rate, particle size of 256 μm, contact angle of 90º and impeller speed of 1300 rpm and minimum attachment angle was 0.13º with 15 L/h air flow rate, particle size of 545 μm, contact angle of 60º and impeller speed of 1300 rpm.

Key Words: Coarse particle, Attachment probability, Collision angle, Attachment angle, Quartz.

INTRODUCTION

The earliest possible recovery of valuable material from a mineral processing circuit could have numerous advantages, such as preventing overgrinding of minerals, reducing flotation time and increasing the recovery of valuable minerals. The decrease in size of the later stages of the circuit will moreover reduce the capital and operating cost of the process, while the energy efficiency of the overall process will improve[1].

†Research and Science Campus, Islamic Azad University, Tehran, Iran.
E-mail: bzshahbazi@yahoo.com

Furthermore, flotation is an extremely complex physico-chemical process. Obviously, a successful bubble-particle attachment is determined by both the chemical nature of the particle surface and the hydrodynamic parameters, such as bubble and particle sizes, the energy of the colliding bubble and particle, and the detachment probability of the bubble-particle couplet[2,3].

Understanding of the various microprocesses involved in the collection of solid particles by air bubbles, namely collision, attachment and detachment, is a fundamental step toward predicting the rate constant of flotation kinetics[4-7].

Unlike the bubble-particle collision microprocess, attachment and detachment strongly depend on the chemistry and physical chemistry of the surface of solid particle and bubble. At present these two microprocesses are the least quantified, because there are many complex phenomena involved which are not well understood yet[8].

In this research, the studies of the influence of impeller speed and air flow rate on flotation performance of particles of quartz has been carried out. Furthermore, probability of particle-bubble attachment, collision angle and attachment angle have also been investigated.

EXPERIMENTAL

Quartz particles (specific gravity = 2.65 g/cm^3) of four diameter classes were used contain: -300+212, -420+300, -500+420 and -590+500 microns. The collector used in the flotation tests was oleic acid (1000 g/ton) at pH = 12.5 and the frother used in the flotation tests was MIBC (75 g/ton). Sodium hydroxide (analytical grade) was used for pH regulation. Anionic flotation of quartz in pH = 12.5 attribute to Ca^{2+} present and activation of quartz surface with this OH^-.

Flotation tests were carried out in a mechanical cell. An impeller diameter of 0.07 meter was used for pulp agitation and a cell with square section was used that its length and height were 0.12 and 0.1 meters, respectively. Impeller rotating speed was 700, 900, 1100 and 1300 rpm and air flow rate was 15, 30, 45 and 75 L/h.

RESULTS AND DISCUSSION

Variation of impeller speed and air flow rate with flotation response of quartz particles: For different air flow rate, the influence of impeller speed on flotation response of quartz particles in four classes are illustrated in Fig. 1. Quartz particles presented a plateau of maximum recovery at 1100 rpm when air flow rate was 15 L/h. For either more quiescent (impeller speed < 1100 rpm) or more turbulent (impeller speed > 1300 rpm) conditions, flotation recovery decreased steadily. This behaviour

suggests that the flotability demands some turbulence to promote particle-bubble collision but that turbulence may not be high enough to destroy particle-bubble aggregates, that other investigators have obtained similar results[9]. The effect of turbulence on particle/bubble attachment and detachment is also found elsewhere[4,10,11].

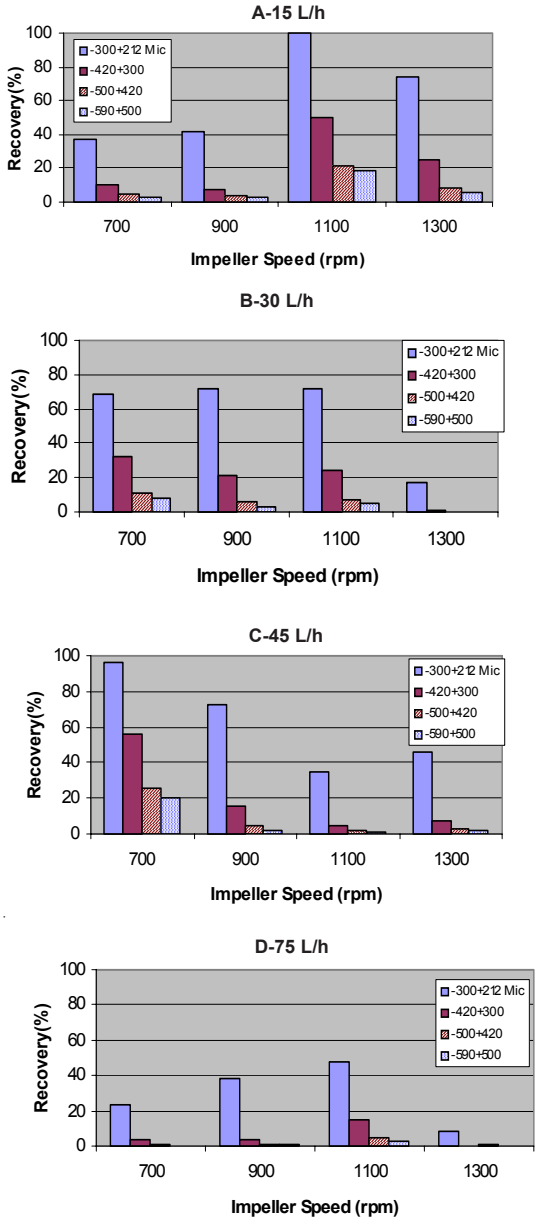

Fig. 1. Flotation response of quartz particles *vs.* impeller speed at various air flow rate

According to Fig. 1, coarse quartz particles showed a pronounced lower recovery than finer ones. It seems that bigger particles demand much more turbulence to become suspended and collide with air bubbles than smaller ones. The results suggest that, regardless of particle size and air flow rate, the aggregates of particle-bubble formed in the pulp, after successful collision and attachment, are likely to be destroyed under the dominance of the severe hydrodynamic conditions characterized by impeller speed = 1100 rpm and flow rate = 15 L/h similar results were obtained by other investigators[9].

A range of 900 < impeller speed < 1100 rpm was explored in flotation tests carried out with *versus* particle sizes and air flow rates. A plateau of maximum recovery was observed at 1100 rpm for impeller speed more than 1300 rpm and no froth layer was observed during flotation experiments and under such a special condition, the recovery was almost nil. In this research, flotation tests carried out in four different flow rates from 15 to 30 and 45 to 75 L/h. The results suggest that with increasing air flow rate flotation recovery decreased to such a level that when air flow rate was around 75 L/h, recovery was found to be minimum.

Bubble size distribution and raise velocity: In this research, bubble size distribution and raise velocity was measured similar to McGill bubble viewer. It consists of a sampling tube attached to a viewing chamber with a window inclined 15º from vertical. Bubble raise into the viewing chamber and are imaged by a digital video camera as they slide up the inclined window illuminated from behind[12]. The mean bubble diameter adopted was the Sauter diameter[13], calculated by the eqn. 1:

$$d_{32} = \frac{\sum n_i d_i^3}{\sum n_i d_i^2} \quad (1)$$

where: n, is number of bubbles and d, is bubble diameter. The effect of impeller speed on Sauter mean bubble diameter at different air flow rate has shown in Fig. 2 and Table-1. The bubble size decreased as impeller speed increased, at the low air flow rate. The effect of air flow rate is shown in Fig. 3 too, as can be seen, bubble size increased with increasing air flow rate.

The effective parameters in bubble Reynolds number are bubble raise velocity, bubble diameter, density and dynamic viscosity of fluid around the bubble. Bubble Reynolds number is calculated[10] from eqn. 2:

$$Re_b = V_b d_b \rho_f / \eta \quad (2)$$

where: V_p is bubble raise velocity, d_b is bubble diameter, η is fluid dynamic viscosity and η_f is fluid density. According to Table-1 and Fig. 3, when air flow rate is 15 L/h, with increasing impeller speed, the bubble raise changes from 16.58 to 14.6, 14.1 and 16.28 cm/s, respectively, but when air flow

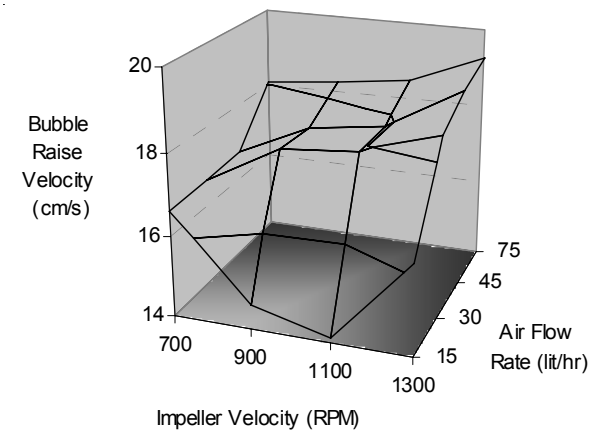

Fig. 2: Effect of the impeller speed on bubble raise velocity at different air flow rates

TABLE-1
BUBBLE SIZE DISTRIBUTION, RAISE VELOCITY AND REYNOLDS NUMBER

Air flow rate (L/h)	Impeller speed (rpm)	Bubble diameter (mm)	Bubble raise velocity (cm/s)	Bubble Reynolds numbers
15	700	1.34	16.58	248
	900	0.83	14.60	135
	1100	0.65	14.1	102
	1300	0.55	16.26	100
30	700	1.02	16.68	190
	900	0.68	17.69	134
	1100	0.69	17.9	138
	1300	0.83	18.47	171
45	700	0.96	16.73	179
	900	0.95	17.58	186
	1100	0.71	17.86	141
	1300	0.82	18.96	174
75	700	1.26	18.02	253
	900	1.21	18.21	246
	1100	1.40	18.45	288
	1300	1.52	19.28	327

rate increased to 30, 45 and 75 L/h increasing impeller velocity cause to increase bubble raise velocity. Minimum bubble raise velocity is 14.1 cm/s around 15 L/h air flow rate and 1100 rpm impeller speed and maximum bubble raise velocity is 19.28 cm/s around 75 L/h air flow rate and 1300 rpm impeller velocity. In this studies, bubble Reynolds numbers changed from 100 to 327.

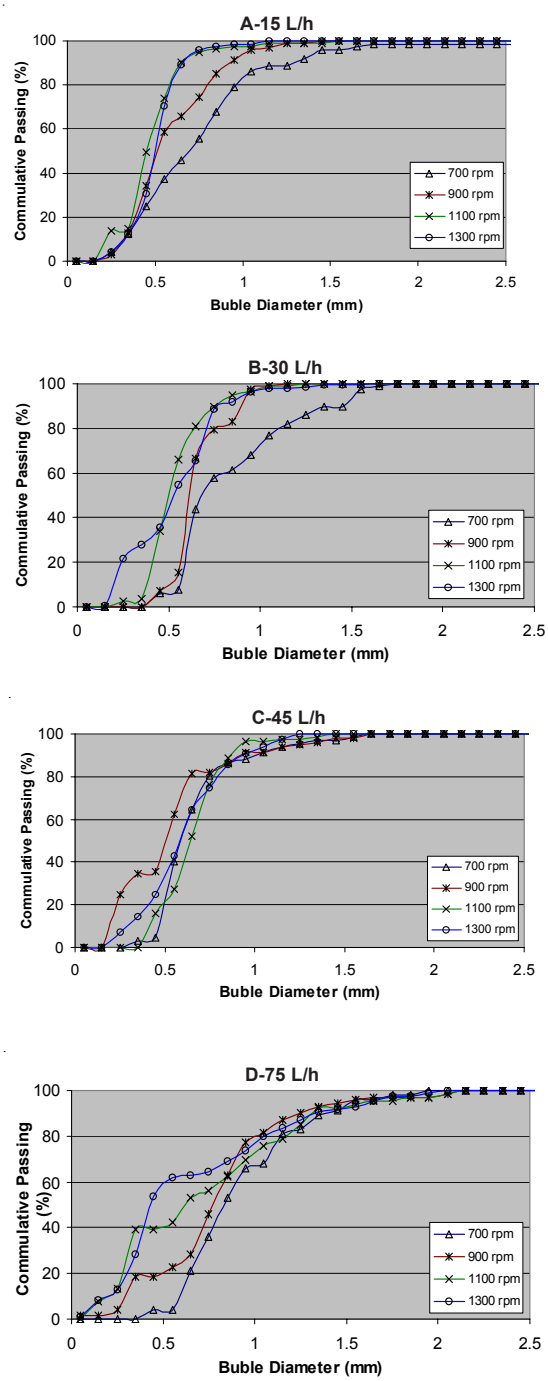

Fig. 3 Effect of the impeller speed on bubble size distribution at different air flow rate

Attachment probability: The probability (P) of a particle being collected by an air bubble in the pulp phase[14] can be given:

$$P = P_c P_{at}(1 - P_d) \tag{3}$$

where, P_c is the probability of bubble particle collision, P_{at} is the probability of adhesion and P_d is the probability of detachment. There is a generalized equation[15] for calculation P_{at} according to eqn. 4:

$$P_{at} = \sec h^2\left(\frac{2UAt_i}{d_p + d_b}\right) \tag{4}$$

where, d_p is the diameter of particle, d_b is the diameter of bubble, t_i is induction time, U is particle settling velocity and A is a dimensionless parameter under Stokes flow:

$$A = \frac{V}{U} + 1 - \frac{3}{4}\left(1 + \frac{d_p}{d_b}\right)^{-1} - \frac{1}{4}\left(1 + \frac{d_p}{d_b}\right)^{-3} \tag{5}$$

where, V is bubble raise velocity. The induction time is a function of the particle size and contact angle which can be determined[16] by experiment and correlated in the form of eqn. 6:

$$t_i = Ad_p^B \tag{6}$$

where parameters A and B are independent of particle size. It was found that parameter B is constant with a value of 0.6 and parameter A is inversely proportional to the particle contact angle θ. On the basis of these findings, the following equation was used[17]:

$$t_i = \frac{75}{\theta} d_p^{0.6} \tag{7}$$

where, t_i is given in second, θ in degrees and d_p in meter. The probability of adhesion can now be calculated for given values of bubble size, particle size and contact angle.

Where neither Newton's nor Stokes' laws apply, there is an equation which can be used[18] for calculation of particle settling velocity (V):

$$V = \frac{20.52\mu_f}{d_p\rho_f}\left(\left[1 + 0.0921\left(\frac{d_p^3(\rho_s - \rho_f)\rho_f g}{0.75\mu_f^2}\right)^{0.5}\right]^{0.5} - 1\right)^2 \tag{8}$$

Fig. 4 shows the P_{at} values predicted using eqn 4. Eqn. 4 suggests that P_{at} is also a function of particle size and bubble size and raise velocity. It has been shown that as the particle size, air flow rate and impeller speed decreases, P_{at} and θ increased. Exceptionally, when air flow rate increases from 45 to 75 L/h, P_{at} increased due to increasing bubble size and raise velocity.

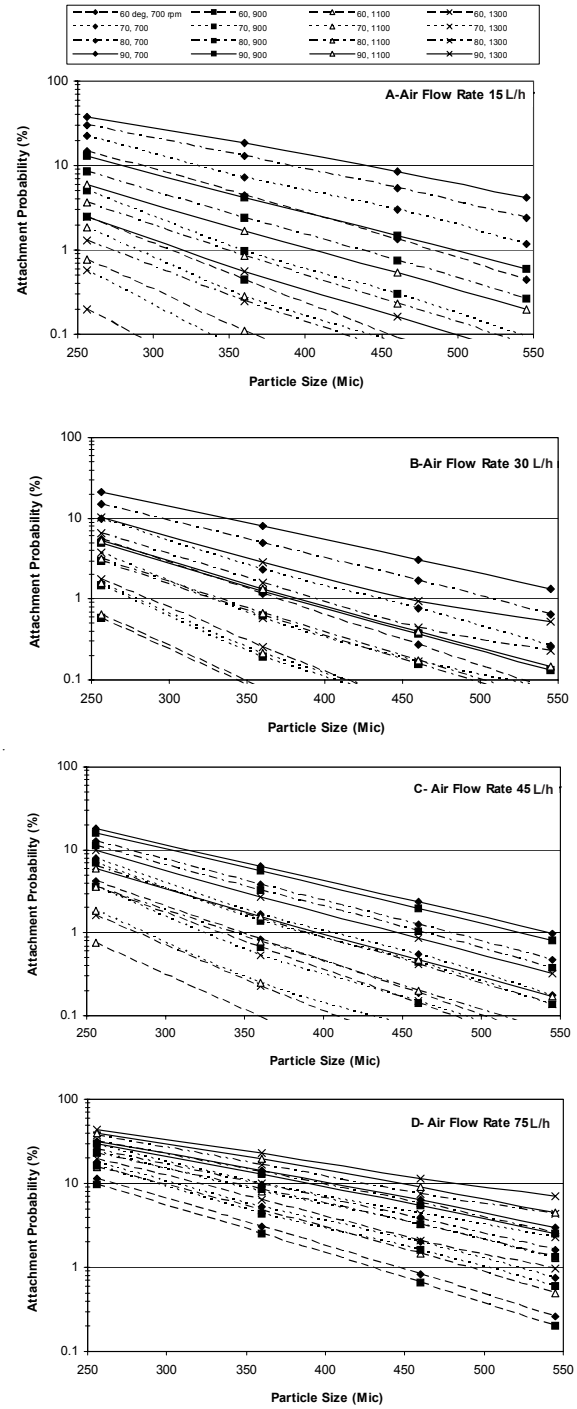

Fig. 4. Attachment probability of coarse particles *vs.* contact angles and air flow rates

Collision and attachment angles: Collision angles has been shown in Fig. 5. The collision angle, ϕ_c, depends weakly on particle size, but strongly on the particle density and the bubble Reynolds number may be predicted[8] by eqn. 9 and used elsewhere[15]:

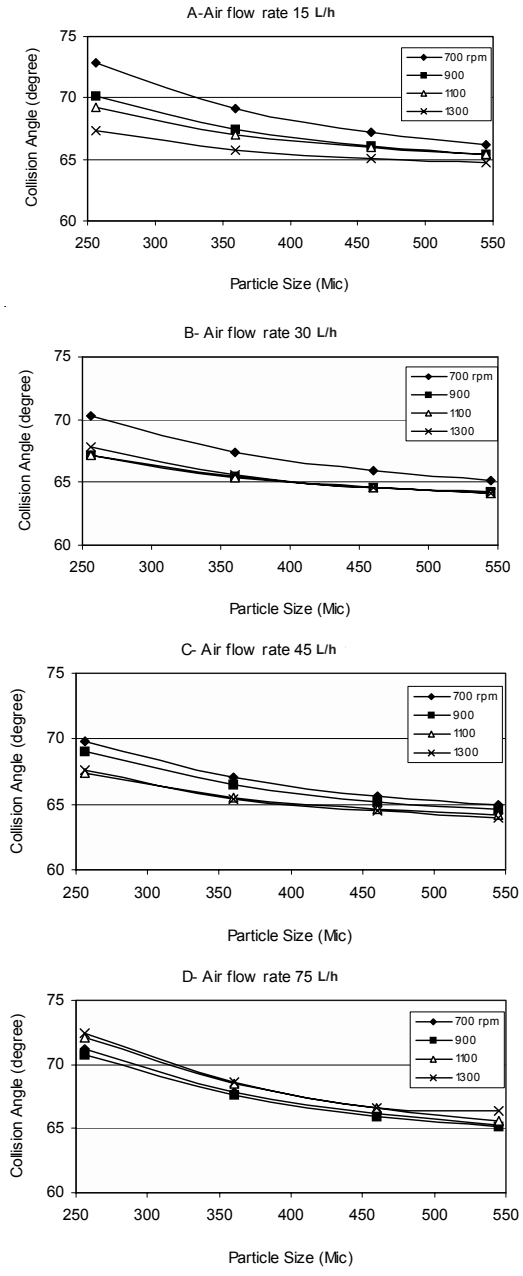

Fig. 5. Collision angle of coarse particles *vs.* contact angles and air flow rates

$$\phi_c = \arccos(D) \tag{9}$$

where the dimensionless parameter D can be calculated[8] using the following eqns. 10-13:

$$X = \frac{3}{2} + \frac{9\,Re}{32 + 9.888\,Re^{0.694}} \tag{10}$$

$$Y = \frac{3\,Re}{8 + 1.736\,Re^{0.518}} \tag{11}$$

$$C = \frac{V}{U}\left(\frac{D_b}{D_p}\right)^2 \tag{12}$$

$$D = \frac{\sqrt{(X+C)^2 + 3Y^2} - (X+C)}{3Y} \tag{13}$$

The bubble-particle attachment probability, P_{at}, is defined as the ratio of these two specific numbers of particles[15]. For calculation of P_{at}, can use[15,19] eqn. 14:

$$P_{at} = \left(\frac{\sin\varphi_{cr}}{\sin\varphi_c}\right)^2 \tag{14}$$

In this research, for various air flow rate, impeller speed and particle size, collision angle has been calculated using eqn. 9. According to Fig. 5 with increasing air flow rate, particle size and impeller speed, collision angle decreases. With decreasing collision angle, sliding time and attachment probability increased. Maximum collision angle was obtained 72.82º with 15 L/h air flow rate, particle size of 256 μm and impeller speed of 700 rpm and minimum collision angle obtained at 64º with 45 L/h air flow rate, particle size of 545 μm and impeller velocity of 1300 rpm.

For prediction attachment angle, ϕ_{cr}, first of all t_i has been calculated using eqn. 7 to be around 60, 70, 80 and 90 degree contact angles and attachment angle has been calculated using eqn. 14. According to Fig. 7 with decreasing air flow rate, particle size and impeller speed, attachment angle increases and with increasing contact angle, attachment angle increased.

Maximum attachment angle was obtained 39.33º with 75 L/h air flow rate, particle size of 256 μm, contact angle of 90º and impeller speed of 1300 rpm and minimum attachment angle was obtained 0.13º with 15 L/h air flow rate, particle size of 545 μm, contact angle of 60º and impeller speed of 1300 rpm.

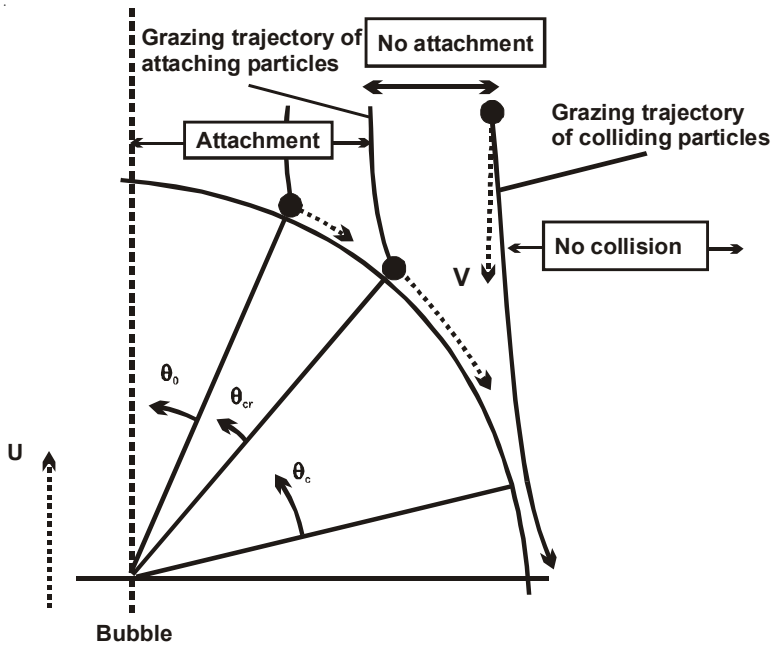

Fig. 6. Bubble- particle collision and attachment interaction in flotation[15]

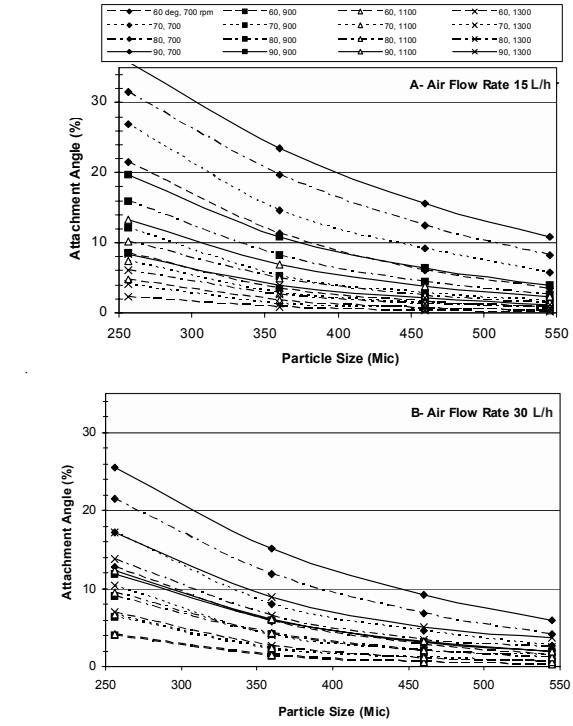

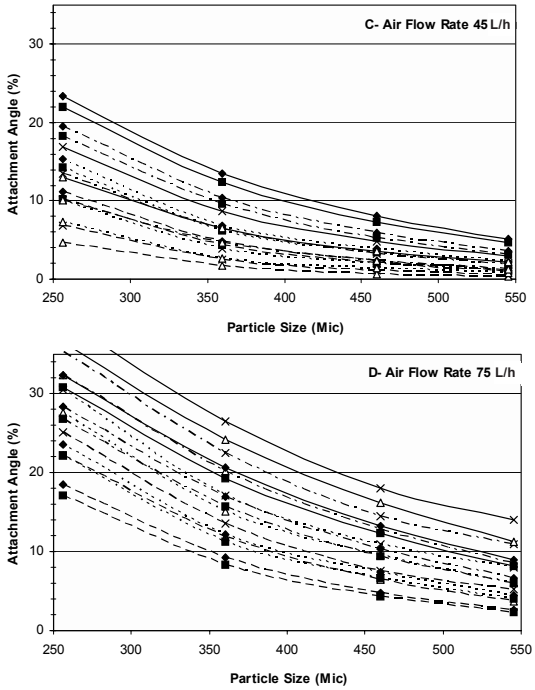

Fig. 7. Attachment angle of coarse particles *vs.* contact angles and air flow rates

Conclusion

In this research, the Bubble-particle attachment probability on coarse particles flotation has been carried out and following conclusions have been drawn:

• Flotation has been carried out in four different flow rates from 15 to 30 and 45 to 75 L/h. The results suggest that with increasing air flow rate flotation recovery decreased to such a level that when air flow rate was 75 L/h recovery was found to be minimum.

• A range of 900 < impeller speed < 1100 rpm was explored in flotation tests carried out *vs.* particle sizes and air flow rates. A maximum recovery was observed at 1100 rpm for impeller speed more than 1300 rpm and no froth layer was observed during experiments and under such a special condition, the recovery was almost nil.

• When air flow rate was 15 L/h, bubble raise changed from 16.58 to 14.60, 14.10 and 16.28 cm/s, respectively, but when air flow rate increased to 30, 45 and 75 L/h increase impeller velocity cause to increase bubble raise velocity.

• Minimum bubble raise velocity was 14.1 cm/s at 15 L/h air flow rate and impeller speed of 1100 rpm and maximum bubble raise velocity was

19.28 cm/s at 75 L/h air flow rate and impeller speed of 1300 rpm. In these tests, bubble Reynolds numbers was changed between 100 to 327.

• For various air flow rates, impeller speed and particle size, collision angle has been calculated. With increasing air flow rate, particle size and impeller speed, collision angle decreased. With decreasing collision angle, sliding time and attachment probability increased.

• Maximum collision angle obtained at 72.82º with 15 L/h air flow rate, particle size of 256 μm and impeller speed of 700 rpm and minimum collision angle was obtained at 64º with 45 L/h air flow rate, particle size of 545 μm and impeller speed of 1300 rpm.

• With decreasing air flow rate, particle size and impeller speed, attachment angle increased with increasing contact angle.

• Maximum attachment angle was obtained at 39.33º with 75 L/h air flow rate, particle size of 256 μm, contact angle of 90º and impeller speed of 1300 rpm and minimum attachment angle was obtained 0.13º with 15 L/h air flow rate, particle size of 545 μm, contact angle of 60º and impeller speed of 1300 rpm.

REFERENCES

1. J.S.J. Denventer, W.A. Dyk, L. Lorenzen and D. Feng, *Minerals Eng.*, **15**, 635 (2002).
2. L. Mao and R.H. Yoon, *Int. J. Miner. Process.*, **51**, 171 (1997).
3. R.H. Yoon and G.H. Luttrel, *Mineral Process. Extrac. Metall. Rev.*, **5**, 101 (1989).
4. H.J. Schulze, in ed.: D.W. Fuerstenau, Physico-Chemical Elementary Processes in Flotation-An Analysis from the Point of View of Colloid Science Including Processes Engineering Considerations, Dev. in Mineral Processing, Vol. 4, Elsevier, Amsterdam, p. 348 (1984).
5. G.S. Dobby and J.A. Finch, *Int. J. Miner. Process.*, **21**, 241 (1987).
6. R. Crawford and J. Ralston, *Int. J. Miner. Process.*, **23**, 1 (1988).
7. D. Hewitt, D. Fornasiero and J. Ralston, *J. Chem. Soc. Farad. Trans*., **91**, 1997 (1995).
8. V.A. Nguyen, *J. Colloid Interface Sci.*, **162**, 123 (1994).
9. W.J. Rodrigues, L.S.L. Filho and E.A. Masini, Hydrodynamic Dimensionless Parameters and Their Influence on Flotation Performance of Coarse Particles, University of Sao Paulo, pp. 1047-1054 (2001).
10. J. Ralston, D. Fornasiero and R. Hayes, *Int. J. Miner. Process.*, **56**, 133 (1999).
11. H. Schubert, *Int. J. Miner. Process.*, **56**, 257 (1999).
12. E.H. Girgin, S. Do, C.O. Gomez and J.A. Finch, *Minerals Eng.*, **19**, 201 (2006).
13. R.T. Rodrigues and J. Rubio, *Minerals Eng.*, **16**, 757 (2003).
14. R.H. Yoon, *Int. J. Miner. Process.*, **58**, 129 (2000).
15. V.N. Anh, J. Ralston and J.S. Hans, *Minerals Eng.*, **53**, 225 (1998).
16. P.T.L. Koh and M.P. Schwarze, *Minerals Eng.*, **19**, 619 (2006).
17. Z. Dai, D. Fornasiero and J. Ralston, *J. Colloid. Interface Sci.*, **217**, 70 (1999).
18. H.K. Bruce, Modeling of Hindered-Settling Column Separations, A Ph.D. Thesis in Mineral Processing, The Pennsylvania State University, pp. 11-13 (2003).
19. J.A. Finch and G.S. Dobby, Column Flotation, Pergamon Press, Oxford, p. 180 (1990).

(*Received*: 2 June 2007; *Accepted*: 28 November 2007) AJC-6100